https://doi.org/10.15407/ujpe63.6.552

P.P. BARDAPURKAR,[1] S.S. SHEWALE,[2] S.A. AROTE,[1] N.P. BARDE[3]

[1] S.N. Arts, D.J.M. Commerce & B.N.S. Science College
*(Sangamner, Maharashtra, India)*
[2] Ahmednagar College
*(Ahmednagar, Maharashtra, India)*
[3] Badrinarayan Barwale Mahavidyalaya
*(Jalna, Maharashtra, India; e-mail: nilesh_ barde123@rediffmail.com)*

# STRUCTURAL AND DIELECTRIC PROPERTIES OF $Ba^{2+}$ SUBSTITUTED LEAD-BARIUM-TITANATE CERAMICS

*Owing to a wide range of applications, ferroelectric ceramics have remained the center of attention of researchers over a large period. With this perception, the present article reports the effects of the substitution of $Ba^{2+}$ in lead titanate (PT) on its structural and electrical properties. X-ray diffractometry was employed for the phase confirmation and to reveal the crystallographic data. It authenticates the single-phase formation with a systematic decrease in the anisotropy. Typical X-ray diffraction data are refined, by using the Rietveld method. The substitution of $Ba^{2+}$ in PT ceramics has caused a reduction in the ferroelectric Curie temperature and significant changes in dielectric properties.*

*K e y w o r d s*: lead titanates, frequency variations, dielectric constant, Curie temperature.

## 1. Introduction

Ferroelectrics are the crystalline substances possessing a permanent spontaneous electric polarization (electric dipole moment per unit volume) that can be reversed by an electric field and are the electrical analog of ferromagnets. A pronounced temperature-dependent Curie temperature, high dielectric constant, low leakage current, low dielectric dispersion, and large P-E hysteresis loop are a few characteristic properties of ferroelectrics to be mentioned. The unique frequency-dependent properties of lead-based ferroelectrics are attributed to the development of nano polar-regions in the vicinity of their transition temperature. These properties make them potential candidates for the application in the field of capacitors, switches, transducers, ferroelectric memories, waveguides, optical memory displays, tunable capacitors, phase shifters, delay lines, ferroelectric-photovoltaic (FE-PV) devices, *etc.* The recent trends in ferroelectric researches are the electrocaloric effect and ferroelectric liquid crystals [1–12].

Perovskite structured oxides have attracted an immense interest due to their prospective applications in electronic components. Perovskite structured ferroelectrics is a class of versatile ferroelectrics, which has a general formula of $ABX_3$; where the cations at the two sites "A" and "B" have different radii ($r_A > r_B$) and "X" is an anion which bonds the two cations. The ratio of cationic species plays a vital role, and the deviations cause distortions in the structural stability. In case of oxides, "$X_3$" is replaced by "$O_3$," and a variety of combinations at "A" and "B" sites are possible with diverse structural properties [13–14].

The present work reports the results of studies on the substitution of $Ba^{2+}$ cations for Pb, i.e. at "A" site of the perovskite structure in the parent compound, which is lead titanate. The following system of a solid solution is formed: $Pb_{1-x}Ba_xTiO_3$, where $x = 0.0$ to $x = 1.0$

The solid state reaction technique was employed for the synthesis. The synthesized samples were characterized by X-ray diffractometry for structural properties. The studies of the dielectric constant as a function of the temperature and the frequency were also carried out.

## 2. Experimental

As mentioned earlier, the samples were synthesized by the ceramic or solid state reaction method, which

involves the pre and final sintering of samples at elevated temperatures.

High purity (purity > 99.9% ) precursors viz. lead oxide (PbO), barium carbonate ($BaCO_3$) and titanium dioxide ($TiO_2$) were mixed in the stoichiometric ratio and then finely ground in an agate mortar-pestle for about 2 h, each. In order to overcome the volatility of lead oxide, 5% excess PbO was added to the mixture. The crushed samples were then pre-sintered at 900 °C for 6 h. This step is intended to crumble the oxides, manage the material shrinkage, and facilitate the homogeneity of the samples. Pre-sintered powders were again finely ground and subjected to the final sintering at 1000 °C to 1200 °C for 8 h. The final sintering assists in a structural reorganization and the diffusion of ions to form the desired product; the mechanism is governed by the Wagner reaction [15] mechanism.

The powder obtained after the final sintering was again ground and then pressed into cylindrical pellets 10 mm in diameter and about 2–3 mm in thickness with a pressure of 6 tons/inch$^2$. Polyvinyl alcohol was used as a binder in the process.

X-ray diffractograms of powder samples were obtained, by using a PW 1830 Philips computerized X-ray diffractometer with $2\theta$ in the range from 20° to 70°. Studies of a variation in the dielectric constant with the temperature and the frequency were carried out, by using an HP 4284-A LCR Q meter in the frequency range 20 Hz to 1 MHz.

## 3. Results and Discussion

### *3.1. Structural*

Figure 1 presents the X-ray diffractograms for all the samples, i.e., for $x = 0.0$ to $x = 1.0$ with a step of 0.25. This has confirmed the single-phase formation of the samples.

All the observed peaks could be indexed to *P4mm* space group with tetragonal symmetry, show a good correspondence with JCPDS card # 60452, and are in good agreement with earlier reports. It can be observed from the diffractogram that there is a gradual shift in the peaks, which reduces the anisotropy of the structure. The parent compound X-ray diffractogram was refined by the Rietveld method, by using the program FullProf [16]. The refined plot is presented in Fig. 2. The plot confirms the single-phase formation, as no secondary phase has been revealed. The refinement was carried out using the Fullprof software. The

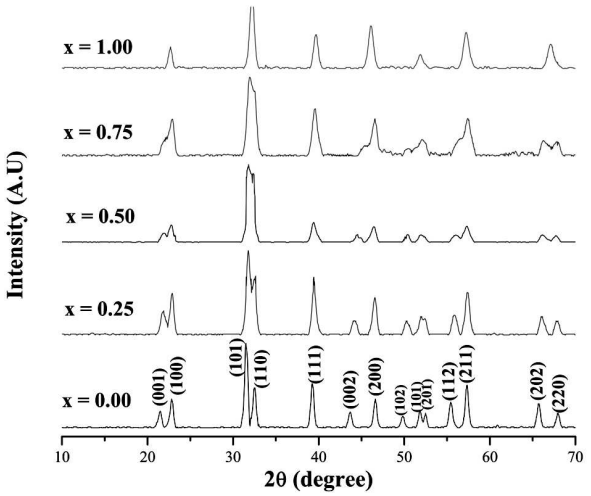


***Fig. 1.*** X-ray diffractograms for all the samples for the system $Pb_{1-x}Ba_xTiO_3$

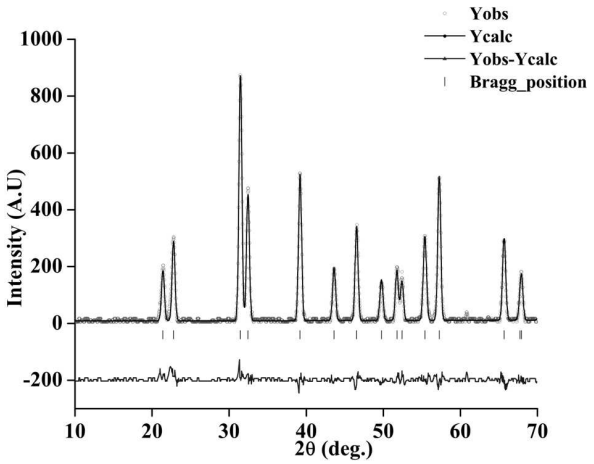


***Fig. 2.*** Results of the Rietveld refinement for the parent compound. The line at the bottom presents the difference between the observed and calculated intensities

*Table 1.* **Lattice anisotropy and particle size for the system $Pb_{1-x}Ba_xTiO_3$**

| Composition | $x = 0.0$ | $x = 0.25$ | $x = 0.50$ | $x = 0.75$ | $x = 1.0$ |
|---|---|---|---|---|---|
| c/a | 1.056 | 1.052 | 1.048 | 1.051 | 1.01 |
| Particle size ($\mu$m) | 132 | 147 | 178 | 201 | 186 |

$R_{wp}$, $R_{exp}$, and $^2$ parameters were found as 25.7, 16.4, and 1.58.

Table 1 gives the lattice anisotropy and particle size (calculated, by using the Scherrer formula), which

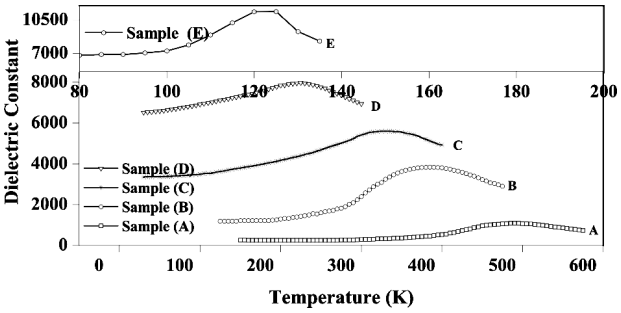


***Fig. 3.*** Variation of the dielectric constant with the temperature at 1 kHz for all the samples

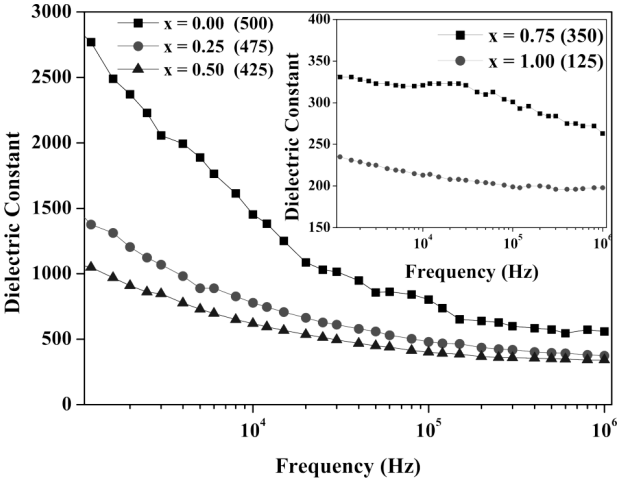


***Fig. 4.*** Variation of the dielectric constant with the frequency for all the samples. (Numbers in bracket indicate the temperature in Celsius degrees

*Table 2.* **Curie temperatures of the samples from dielectric measurements for the system $Pb_{1-x}Ba_xTiO_3$**

| Composition | $x = 0.0$ | $x = 0.25$ | $x = 0.50$ | $x = 0.75$ | $x = 1.0$ |
|---|---|---|---|---|---|
| $T_c$ (°C) | 485 | 405 | 330 | 220 | 125 |

shows that the particle size increases with the dopant concentration. A reduction in the lattice anisotropy may be attributed to the incorporation of $Ba^{+2}$ ions at $Pb^{+2}$ sites and is consistent with the earlier report [17].

### *3.2. Dielectric measurement*

#### *3.2.1. Temperature dependence*

The samples were studied for their dielectric properties. The variations of the dielectric constant with the temperature for all the samples are represented in Fig. 3. The variation of the dielectric constant with the temperature shows a typical behavior for all the samples. It increases initially with the temperature, attains a maximum at a certain temperature, and then falls down.

All these measurements are taken at a constant frequency of 1 kHz. The temperature, at which the dielectric constant attains the peak, is known as the Curie or transition temperature for a particular sample. This transition indicates that the samples have undergone the ferroelectric to paraelectric phase transition at the transition temperature [18]. When the interfacial polarization dominates the dipolar polarization, the typical rise in the dielectric constant with the temperature up to the transition is observed [19]. This indicates the supremacy of the interfacial polarization in the present samples.

The addition of $Ba^{2+}$ affects the ferroelectric interactions and consequently the electric polarization of the samples. As the temperature is changed, the internal structure of the material undergoes certain changes, by causing a change in the dielectric constant. Thus, as the $Ba^{2+}$ content increases, the transition temperature is found to decrease linearly. Table 2 presents the transition temperatures for all the samples, determined from dielectric studies.

The temperature interval in the vicinity of the Curie point is associated with the Curie temperature of a fraction or microregions of the entire volume. The microregions are distributed below and above the Curie temperature. The Curie point region can be sharp in some ferroelectrics, whereas it can be broad maxima in relaxor ferroelectrics. The Curie region width is sensitive to the compositional fluctuations. In the present case, the region around the dielectric maxima is found to be broadened, by suggesting a diffused phase transition, which can be ascribed to the co-existence of the ferroelectric and paraelectric regions (co-existence of microregions) in the vicinity of the transition temperature [20]. The inter ionic distances are temperature-dependent. An increase in the thermal energy compels the ions to separate. This results in a reduction of the dipolar polarization. The variation of the dielectric constant shows a typical behavior: a rise up to the transition temperature and a fall after this temperature. A decrease in the dielectric constant can be attributed to a swift defeat of the polarization in the material due

to thermal effects. The dielectric constant follows the Curie–Weiss law $\varepsilon' C/(T-T_0)$ near the Curie temperature, in which $C$ is the Curie–Weiss constant, and $T_0$ is the Curie–Weiss temperature [21].

*3.2.2. Frequency dependence*

Variations of the dielectric constant with the frequency for all the samples are represented in Fig. 4. It shows a typical behavior for all the samples, i.e., a decreasing trend with increase in the frequency. The interfacial polarization is frequency-dependent and decreases with a rise in the frequency. The creation of crystal defects results in an increase in the interfacial polarization [22, 23].

The plots show that the dielectric constant has a negative exponential relation to the applied frequency. This can easily be explained on the basis of the behavior of electrical dipoles. If the dipoles could cope up with the applied field, i.e., if they could flip with the same frequency, there won't be any dielectric loss. However, in the real-time case, the dipoles have certain inertia and cannot switch their orientation with the applied signal, which results in the observed decay [24]. However, at substantially higher frequencies, the variation is almost constant, by indicating that the synthesized samples can be potential candidates for high-frequency applications, and an appropriate material can be synthesized to suit the specific requirements.

## 4. Conclusions

Structural studies on the $Pb_{1-x}Ba_xTiO_3$ system shows the strong effect of the substitution of $Ba^{2+}$ on the properties of lead titanate. XRD patterns show the single-phase formation with a tetragonal structure for all the samples. The lattice anisotropy (c/a ratio) is found to decrease with increasing the $Ba^{2+}$ content. The variation of the dielectric constant with the temperature shows a hump at the ferroelectric-to-paraelectric phase transition temperature, indicating a diffused phase transition (DPT). Thus, the substitution of $Ba^{2+}$ in PT is found to lower the Curie temperature and the anisotropy significantly. The dielectric constant is found to decrease exponentially with the frequency and to attain an almost constant level at higher frequencies, by indicating a potential candidature of the material for high-frequency applications. The dielectric constant is thus found to be significantly modified with the $Ba^{2+}$ addition. These changes in the structural and dielectric properties by the substitution of $Ba^{2+}$ may be useful for the applications in the field of transducers, high-frequency applications, informatics, piezoelectric actuators *etc.*


1. O. Mojca, R. Angelika, R. Klaus. Electric field-induced changes of domain structure and properties in La-doped PZT–from ferroelectrics towards relaxors. *J. Eur. Ceram. Soc.* **36**, 2495 (2016).
2. Zhi Ma, Yanan Ma, Zhipeng Chen, Fu Zheng, Hua Gao, Hongfei Liu, Huanming Chen. Modeling of hysteresis loop and its applications in ferroelectric materials, **44** (4), 4338 (2018).
3. Bingcheng Luo, Xiaohui Wang, Enke Tian, Hongzhou Song, Haimo Qu, Ziming Cai, Baiwen Li, Longtu Li. *Mechanism of ferroelectric properties of (BaCa)(ZrTi)$O_3$ from first principles calculations.* (Ceramics International, Available online 2, 2018).
4. Xiaomeng Ma, Sanshan Li, Yanyan He, Ting Liu, Yebin Xu. The abnormal increase of tunability in ferroelectric-dielectric composite ceramics and its origin. *J. Alloys and Compounds* **739**, 755 (2018).
5. Yongbo Yuan, Zhengguo Xiao, Bin Yang, Jinsong Huang. Arising applications of ferroelectric materials in photovoltaic devices. *J. Mater. Chem. A* **2**, 6027 (2014).
6. Yang Bai. Influence of microstructure features on electrocaloric effect in ferroelectric ceramics. *Ceramics International* **44** (7), 8263 (2018).
7. S. Shoarinejad, R. Mohammadi Siahboomi, M. Ghazavi. Theoretical studies of the influence of nanoparticle dopants on the ferroelectric properties of a ferroelectric liquid crystal. *J. Molecular Liquids* **254**, 312 (2018).
8. Hyun Wook Shin, Jong Yeog Son. Asymmetric ferroelectric switching characteristics of ferroelectric poly (vinylidene fluoride-ran-trifluoroethylene) thin films grown on highly oriented pyrolytic graphite substrates. *Organic Electronics* **51**, 458 (2017).
9. *Ferroelectrics – Applications.* Edited by M. Lallart (InTech, 2011).
10. Online resources. http://www.indiastudychannel.com /resources/117961-Ferroelectric-Materials-Theory-Properties-and-applications.aspx, accessed on (27 Aug 2017).
11. Online resources. https://www.azom.com/article.aspx?ArticleID=3593#, accessed on (27 Aug 2017).
12. Online resources. https://www.electrical4u.com/ferroelectric-materials/, accessed on (27 Aug 2017).
13. Dong Hou, Changhao Zhao, A.R. Paterson, Shengtao Li, J.L. Jones. Local structures of perovskite dielectrics and ferroelectrics via pair distribution function analyses. *J. Europ. Ceramic Society* **38** (4), 971 (2018).
14. T. Shi, G. Li, J. Zhu. Compositional design strategy for high performance ferroelectric oxides with perovskite structure. *Ceramics International* **43** (3), 2910 (2017).

15. H. Yurtseven, A. Kiraci. Temperature dependence of the polarization and the dielectric constant near the paraelectric-ferroelectric transitions in $BaTiO_3$. *J. Mol. Model* **19**, 3925 (2013).
16. J. Rodriguez-Carvajal, T. Roisnel. FullProf.98 and WinPLOTR: New Windows 95/NT applications for diffraction commission for powder diffraction, international union for crystallography, Newletter No. 20 (May-August) (Summer 1998).
17. P.P. Bardapurkar, N.P. Barde, D.P. Thakur, K.M. Jadhav, G.K. Bichile. Effect of $Ba^{2+}$–$Sr^{2+}$ co-substitution on the structural and dielectric properties of lead titanate. *J. Electroceram* **29**, 62 (2012).
18. Wei Hu. *Experimental search for high Curie temperature piezoelectric ceramics with combinatorial approaches*. Graduate thesis and dissertation (Iowa State University Ames, 2011).
19. Online resources, http://nptel.ac.in/courses/113104005/lecture18a/18_2.htm, accessed on (27 Aug 2017).
20. Yaru Wang, Yongping Pu, Xin Li, Hanyu Zheng, Ziyan Gao. Evolution from ferroelectric to diffused ferroelectric and relaxor ferroelectric in $BaTiO_3$–$BiFeO_3$ solid solutions. *Mater. Chem. Phys.* **183**, 247 (2016).
21. O.P. Thakur, Chandra Prakash, D.K. Agrawal. Dielectric behavior of $Ba_{0.95}Sr_{0.05}TiO_3$ ceramics sintered by microwave. *Mater. Sci. Eng. B* **96**, 221 (2002).
22. Gupta Vineeta, K.K. Bamzai, P.N. Kotru, B.M. Wanklyn. Dielectric properties, ac conductivity and thermal behavior of flux grown cadmium titanate crystals. *Mater. Sci. Eng. B* **130**, 163 (2006).
23. K. Singh Amarendra, T.C. Goel, R.G. Mendiratta. Dielectric properties of Mn-substituted Ni–Zn ferrites. *J. Appl. Phys.* **91**, 6626 (2002).
24. R. Balusamy, P. Kumaravel, N.G. Renganathan. Dielectric and electrical properties of lead zirconate titanate. *Der Pharma Chemica* **7** (10), 175 (2015).

Received 20.03.18

*П.П. Бардапуркар, С.С. Шевальє,*
*С.А. Арote, Н.П. Барді*

СТРУКТУРНІ І ДІЕЛЕКТРИЧНІ ВЛАСТИВОСТІ КЕРАМІКИ З ТИТАНАТУ СВИНЦЮ ІЗ ЗАМІЩЕННЯМ $Ba^{2+}$

Р е з ю м е

Завдяки широкій області застосування, кераміки-ферроелектрики залишаються в центрі уваги дослідників. В даній роботі вивчається ефект заміщення барієм $Ba^{2+}$ в титанаті свинцю на його структуру і електричні властивості. Рентгенівська дифрактометрія з використанням методу Ритвельда застосована для визначення фазового складу і кристалографічних параметрів. Показано утворення однієї фази і систематичне зменшення анізотропії. Заміщення барієм $Ba^{2+}$ в титанаті свинцю зменшує температуру Кюрі ферроелектрика і істотно змінює його діелектричні властивості.